Multipole decomposition of the elastic atomic photon scattering form factor and the anomalous scattering factor

2006 J. Phys. A: Math. Gen. 39 5089

(http://iopscience.iop.org/0305-4470/39/18/022)

INSTITUTE OF PHYSICS PUBLISHING JOURNAL OF PHYSICS A: MATHEMATICAL AND GENERAL

J. Phys. A: Math. Gen. **39** (2006) 5089–5103 doi:10.1088/0305-4470/39/18/022

Multipole decomposition of the elastic atomic photon scattering form factor and the anomalous scattering factor

L A LaJohn

Department of Physics and Astronomy, University of Pittsburgh, Pittsburgh, Pennsylvania 15260, USA

Received 21 February 2006
Published 19 April 2006
Online at stacks.iop.org/JPhysA/39/5089

Abstract

The elastic atomic photon scattering form factor amplitude A^{f0}, obtained from the high energy and low momentum transfer (**K**) limit of the exact (within the independent particle approximation (IPA)) Rayleigh relativistic second order S-matrix scattering amplitude A^{sm} is decomposed into an infinite sum of its electric and magnetic field multipoles. The energy-dependent part of A^{f0} (the scattering angle-dependent part of A^{f0} is incorrect due to the low **K** approximation), combined with the angle-dependent part of A^{sm}, yields a form factor amplitude A^{f} (different versions of A^{f} and A^{f0} will be described in the text) that can be used to decompose the anomalous scattering factor A^{asf} into its multipoles. A^{f0} which initially contains coherent and incoherent factors is reduced to a single sum over the multipoles of only coherent terms by assuming that the charge density is spherically symmetric. At photon energies up to about ten times the K-shell binding energy it takes up to quadrupole A^{asf} for light atoms of $Z \leqslant 20$ and up to the fourth multipole for heavy atoms such as uranium for an accurate A^{asf} (within IPA). The multipole contributions were found to become somewhat larger as the scattering angle becomes larger (greater than 120°); however there were partial cancellations of such effects.

PACS number: 32.80.Cy

1. Introduction

Rayleigh scattering is a process in which photons are scattered off bound electrons with no loss of photon energy (the frequency of the incident and scattered photon are the same). This process is named after Lord Rayleigh (John William Strutt), who explained the blue colour of the sky in terms of preferential scattering of short wavelength sunlight by molecules in the upper atmosphere. Even though Rayleigh scattering is an elastic process, momentum is transferred to the atom if the direction of the photon is altered by collision with the atom.

The collision causes bound electrons to be promoted to higher levels, but the atom returns to its initial state when the process is completed. Rayleigh scattering can be used to probe the electronic properties of atoms, molecules and materials. It is also a very useful tool in medical research and diagnostics.

Theoretical Rayleigh scattering cross sections (including differential cross sections) are obtained from a matrix element A^R. An exact value for A^R can be obtained in principle from the theory of relativistic quantum electrodynamics. An exact A^R within the independent particle approximation (IPA) has been obtained from second order S-matrix theory. The corresponding matrix element $A^{\rm sm} = A_a^{\rm sm} + A_e^{\rm sm}$ is composed of two sets of integral terms each summed over all excited states, one corresponding to an absorption first $A_a^{\rm sm}$ the other to emission first $A_e^{\rm sm}$ scattering diagram (see for example [1, 2] for further details and discussion). The S-matrix formalism was later extended to fourth order perturbation in order to include the most important electron–electron correlation diagrams for a two electron atom or ion [3]. Kissel *et al* [4] created a rather extensive code based on the Dirac–Slater potential for computing Rayleigh differential cross sections within IPA for photon energies ranging from 100 eV to 10 MeV. However, since the formalism the code is based on includes a multipole expansion of the vector potential, the number of multipoles required for an accurate $A^{\rm sm}$ increases with increasing photon energy. In order to save computation time and avoid convergence problems when calculating whole atom cross sections, the approach was to obtain outer shell contributions to the amplitude using form factors, then use S-matrix theory to get the inner shell contributions.

Some of the various approximate theoretical methods for the computation of Rayleigh scattering differential cross sections include the form factor, a modification of the form factor and the form factor (or modified form factor) plus the anomalous scattering factor. These methods were evaluated by comparison to the more accurate S-matrix values [5]. The form factor $f(q)$, which is exact only in the case of ${}^1S_0$, is given by

$$f(q) = 4\pi \sum_p \int_0^\infty H_p(r)\rho_p(r)\left[\frac{\sin(qr)}{qr}\right] r^2\,{\rm d}r, \tag{1}$$

$\rho_p(r)$ is the charge density for the subshell p, q is the magnitude of the photon momentum transfer where, $q = h^{-1}|\mathbf{K_i} - \mathbf{K_f}|$ with $\mathbf{K_i}$ and $\mathbf{K_f}$ the momentum vectors for the incident and scattered photons respectively and $H_p(r) = 1$. In the modified form factor as described in [5], $H_p(r) = [|E_p| - V(r)]^{-1}$, ($E_p$ is the binding energy for an electron in the subshell p, $V(r)$ is the potential). Here $H_p(r)$ includes some of the electron nuclear Coulomb effects. A better approximate method involves addition of a correction to the form factor (or modified form factor) called the anomalous scattering factor. The corresponding amplitude for this correction $A^{\rm asf}$ is defined as the difference between the exact Rayleigh amplitude and the high energy limit of the Rayleigh amplitude. $A^{\rm asf}$ is given by the sum of a real and imaginary amplitude, where in the case of forward angle scattering, the imaginary amplitude is proportional to the corresponding photoeffect cross section $\sigma_{\rm ph}$ resulting from the optical theorem, while the real component is a function of the imaginary one due to a dispersion relationship [5–7]. $A^{\rm asf}$ can be obtained for forward angle scattering from $\sigma_{\rm ph}$ at energies below $2mc^2$ and at energies at which resonances do not occur.

Even though $A^{\rm asf}$ is not strongly scattering angle dependent, such $A^{\rm asf}$ values obtained from $\sigma_{\rm ph}$ still become progressively less accurate with increasing angle. An angle-dependent version of $A^{\rm asf}$ was derived from a nonrelativistic Coulombic function that includes corrections beyond the dipole amplitude for the K-shell case [8, 9]. Decomposition of a relativistic $A^{\rm asf}$ by taking the difference between $A^{\rm sm}$ and A^f at corresponding multipoles and subshells (i.e. $A^{\rm asf} = \sum_{pj}\left[A_{pj}^{\rm sm} - A_{pj}^f\right]$ (j is the 2^jth pole) can provide a useful guide to anyone who

is interested in deriving an angle-dependent A^{asf} that would go beyond the K-shell and be accurate for any atom. Here one could assess the magnitude of each multipole contribution to the elastic scattering amplitude for each subshell in a given energy regime and make comparisons to any newly derived results. One would expect the multipole requirements of A^{asf} to be similar to that for σ_{ph} [10] at forward angle; however nothing is known about the multipole requirements of A^{asf} at finite angles.

The calculations presented in this paper were done within IPA using a Dirac–Slater potential. This model is generally good at high photon energies even though it is now understood that electron–electron correlation contributions can be significant at these energies for non-s states as was shown to be the case for photoeffect [11]. However it was later found that net correlation contributions are generally small due to partial cancellation of such effects [12]. Clearly IPA results would not include contributions such as those due to giant resonances which are strongly dependent on electron–electron correlations and relaxation effects such as for example that described in [13].

In the work presented in this paper, the form factor amplitude obtained from the high energy low momentum transfer limit of the S-matrix amplitude is decomposed into electric and magnetic field multipoles. $f(q)$ as given by equation (1), which can be factored out from A^f, will be referred to as the form factor (not an amplitude). $f(q)$ is proportional to the scattering amplitude for the case of polarization perpendicular to the scattering plane, designated by $A^f_\perp = -r_0 f(q)$, while the total form factor amplitude for elastic scattering is given by $A^f = A^f_\perp[1 + \cos(\theta)]$ (see p 80 in [14]). The multipole decomposed A^{sm} and A^f amplitudes will be used to obtain the multipole decomposed anomalous scattering amplitude A^{asf}. This work, along with providing a useful guide for the extension of finite angle scattering A^{asf} to heavy atoms, will hopefully enhance ones understanding of the relationships between the form factor and S-matrix expressions for elastic photon scattering amplitudes.

2. Theory and formalism

2.1. S-matrix formalism and some relevant definitions

The expression for the elastic (Rayleigh) S-matrix element in the limit of high photon energy and low momentum transfer $\mathbf{K}$ is given by (see [5, 15] also see appendix A)

$$A^{\mathrm{sm}} \simeq r_o[\varepsilon_{\mathbf{i}} \cdot \varepsilon^*_{\mathbf{f}}] \sum_p \left\langle p \left| \frac{\mathrm{e}^{-\mathrm{i}\mathbf{K}\cdot\mathbf{r}}}{|E_p| - V - c(\bar{\mathbf{K}} \cdot \mathbf{P})} \right| p \right\rangle, \tag{2}$$

where $m = c = 1$. Assuming low $\mathbf{K}$, the form factor amplitude A^{f0} (A^{f0} includes both the modified and unmodified form factor amplitudes throughout this paper) results if $c(\bar{\mathbf{K}} \cdot \mathbf{P})$ is omitted yielding

$$A^{f0} = -r_o[\varepsilon_{\mathbf{i}} \cdot \varepsilon^*_{\mathbf{f}}] \sum_p \int \rho_p(\mathbf{r}) H_p(r) \exp(-\mathrm{i}\mathbf{K} \cdot \mathbf{r})\, \mathrm{d}\tau. \tag{3}$$

Here ε_i and ε_f are the polarization vectors for the incident and scattered photon respectively and r_0 is the classical electron radius. The sum is over atomic subshells p, each designated by a set of quantum numbers n, m and κ (κ is the relativistic quantum number defined as $\kappa = \mp(j_p + 1/2)$ with $j_p = l \pm 1/2$), $\mathbf{P}$ is the electron momentum vector, for small momentum transfer $\bar{\mathbf{K}} = \mathbf{K_i} \approx \mathbf{K_f}$. $H_p = [|E_p| - V(r)]^{-1}$ for the modified form factor and $H_p = 1$ for the unmodified form factor amplitudes.

The exponent in equation (3) can be expanded as a product of two plane waves, one for the incident the other for the scattered photon, doubly summed over j and M,

$$[\hat{\varepsilon}_i\hat{\varepsilon}_f^*]\exp(-\mathrm{i}\mathbf{K}\cdot\mathbf{r}) = \sum_{jM\lambda}\sum_{j'M'}(-1)^{j+j'}\left[\mathbf{a}^{\lambda}_{\mathbf{jM}}(\mathbf{r})\cdot\mathbf{a}^{\lambda}_{\mathbf{j'M'}}(\mathbf{r})\right]\left[C^{\lambda}_{jM}(\mathbf{K_i})C^{\lambda}_{j'M'}(\mathbf{K_f})\right], \tag{4}$$

where the vector potential $\mathbf{a}^{\lambda}_{\mathbf{jM}}$, is of multiplicity λ, such that the magnetic field corresponds to $\lambda = 0$ and the electric field to $\lambda = 1$, j is the multipolarity (2^j-pole, $j \geqslant 1$, an integer) and M is the total angular momentum. Unprimed subscripts refer to the incident photon (initial photon state), primed to scattered photon (final photon state). Here

$$\begin{aligned}\mathbf{a}^{\mathbf{0}}_{\mathbf{jM}}(\mathbf{r}) &= j_j(kr)\mathbf{Y}_{\mathbf{jjM}}(\mathbf{r})\\ \mathbf{a}^{\mathbf{1}}_{\mathbf{jM}}(\mathbf{r}) &= \left(\frac{j+1}{2j+1}\right)^{1/2} j_{j-1}(kr)\mathbf{Y}_{\mathbf{jj-1M}}(\mathbf{r}) - \left(\frac{j}{2j+1}\right)^{1/2} j_{j+1}(kr)\mathbf{Y}_{\mathbf{jj+1M}}(\mathbf{r}),\end{aligned} \tag{5}$$

where $j_l(kr)$ is a spherical Bessel function and $\mathbf{Y}_{\mathbf{jlm}}(\hat{\mathbf{r}})$ is the angular momentum vector spherical harmonics (VSH) in which $l = j \pm 1$ for the electric field and $l = j$ for the magnetic field. The scattering angle-dependent part of the plane waves for $\lambda = 0, 1$ is given by

$$\begin{aligned}C^0_{jM}(\mathbf{K}) &= \mathbf{Y}_{\mathbf{jjM}}(\mathbf{K})\cdot\hat{\varepsilon}\\ C^1_{jM}(\mathbf{K}) &= \left[\left(\frac{j}{2j+1}\right)^{1/2}\mathbf{Y}_{\mathbf{jj+1M}}(\mathbf{K}) + \left(\frac{j+1}{2j+1}\right)^{1/2}\mathbf{Y}_{\mathbf{jj-1M}}(\mathbf{K})\right]\cdot\hat{\varepsilon}\end{aligned} \tag{6}$$

[1, 5], where $\hat{\varepsilon}$ is the unit polarization vector. $\mathbf{Y}_{\mathbf{jlM}}(\mathbf{K})$ is given by

$$\mathbf{Y}_{\mathbf{jlM}}(\mathbf{K}) = \sum_{mq} Y_{lm}(K)\hat{\varepsilon}_{\mathbf{q}}(lm1q|l1jM), \tag{7}$$

where $q = 0, \pm 1$, $m + q = M$, $\hat{\varepsilon}_{\pm\mathbf{1}} = \mp\left(\frac{1}{2}\right)^{1/2}([\varepsilon_x] \pm \mathrm{i}[\varepsilon_y])$ and $\hat{\varepsilon}_{\mathbf{0}} = \varepsilon_z$: $(lm1q|l1jM)$ is the vector coupling coefficient (VCC) [16].

2.2. An expression for A^{f0} having coherent and incoherent terms doubly summed over both multipoles and angular momentum

The form factor amplitude in spherical polar coordinates is given by

$$\begin{aligned}{}^{\mathrm{mag}}A^{f0}(\mathbf{K}) = -r_0[\varepsilon_i\varepsilon_f]&\sum_{jj'MM'p}(-1)^{j+j'}\left[V_{pjj'}(E)W^p_{jj'jj'MM'}\right]\\ &\times[\mathbf{Y}_{\mathbf{jjM}}(\mathbf{K_i})\cdot\hat{\varepsilon}_{\mathbf{i}}][\mathbf{Y}_{\mathbf{j'j'M'}}(\mathbf{K_f})\cdot\hat{\varepsilon}_f]\end{aligned} \tag{8}$$

for the magnetic field and

$$\begin{aligned}{}^{\mathrm{el}}A^{mf0}(\mathbf{K}) = -r_0[\varepsilon_i\varepsilon_f]\sum_{jj'MM'p}(-1)^{j+j'}&\left\{\left[\left(\frac{j+1}{2j+1}\right)^{1/2}\left(\frac{j'+1}{2j'+1}\right)^{1/2}V_{pj-1j'-1}(E)\right.\right.\\ &\times W^p_{jj'j-1j'-1MM'} - \left(\frac{j}{2j+1}\right)^{1/2}\left(\frac{j'+1}{2j'+1}\right)^{1/2}V_{pj+1j'-1}(E)W^p_{jj'j+1j'-1MM'}\\ &- \left(\frac{j+1}{2j+1}\right)^{1/2}\left(\frac{j'}{2j'+1}\right)^{1/2}V_{pj-1j'+1}(E)W^p_{jj'j-1j'+1MM'}\\ &\left.\left.+\left(\frac{j}{2j+1}\right)^{1/2}\left(\frac{j'}{2j'+1}\right)^{1/2}V_{pj+1j'+1}(E)W^p_{jj'j+1j'+1MM'}\right]\right.\end{aligned}$$

$$\times \left\{ \left[\left(\frac{j}{2j+1} \right)^{1/2} \mathbf{Y_{jj+1M}(K_i)} + \left(\frac{j+1}{2j+1} \right)^{1/2} \mathbf{Y_{jj-1M}(K_i)} \right] \right.$$
$$\left. \times \hat{\varepsilon}_{\mathbf{i}} \left[\left(\frac{j'}{2j'+1} \right)^{1/2} \mathbf{Y_{j'j'+1M'}(K_f)} + \left(\frac{j'+1}{2j'+1} \right)^{1/2} \mathbf{Y_{j'j'-1M'}(K_f)} \right] \cdot \hat{\varepsilon}_{\mathbf{f}} \right\} \quad (9)$$

for the electric field. Here E is the photon energy, and $V_{pll'}(E)$ represents the radial integrals for an electron in subshell p and is given by

$$V_{pll'}(E) = \int_0^\infty \rho_p(r) H_p(r) j_l(kr) j_{l'}(kr) r^2 \, \mathrm{d}r, \quad (10)$$

where $\rho_p(r)$ contains radial wavefunctions designated by $|n\kappa m\rangle$. The angular momentum integral for the subshell p is given by

$$W^p_{jj'll'MM'} = \int_0^\pi \int_0^{2\pi} \mathbf{Y_{jlM}}(\theta, \phi) \cdot \mathbf{Y_{j'l'M'}}(\theta, \phi) \Omega_p^2(\theta, \phi) \sin\theta \, \mathrm{d}\theta \, \mathrm{d}\phi. \quad (11)$$

Here $\Omega_p(\theta, \phi)$ is composed of the VCC, the spherical harmonics and a spinor corresponding to the subshell p.

2.3. Reduction of the expression for A^{f0} to one having a single multipole sum over only coherent terms

A^{f0}, based on equations (8) and (9), is given as a double sum over j and M, which includes coherent and incoherent terms. If one assumes that the charge density is spherically symmetric, thereby setting $\Omega_p(\theta, \phi) = 1$ in equation (11), equations (8) and (9) reduce to much simpler expressions. Here $W^p_{jj'll'MM'}$ reduces to $W_{jj'll'MM'}$, which is equal to a product of Kronecker deltas

$$W_{jj'll'MM'} = \int_0^\pi \int_0^{2\pi} \mathbf{Y_{jlM}}(\theta, \phi) \cdot \mathbf{Y_{j'l'M'}}(\theta, \phi) \sin\theta \, \mathrm{d}\theta \, \mathrm{d}\phi = \delta_{jj'} \delta_{ll'} \delta_{MM'}, \quad (12)$$

and the radial integral in these two equations is now given by

$$V_{pl}(E) = \int_0^\infty \rho_p(r) H_p(r) j_l^2(kr) r^2 \, \mathrm{d}r. \quad (13)$$

The angle-dependent part of equations (8), (9) are simplified by placing the incident photon on the z-axis with scattering on the x–z plane. This can be achieved by starting with $Y_{jlM}(\bar{\theta}, \bar{\phi})$, where $\bar{\theta}$ is the angle between either the incident or scattered photon and the z-axis and $\bar{\phi}$ is the azimuthal angle about the x–y plane (bar signifies experimental geometry). Setting the azimuthal angle, $\bar{\phi} = 0^\circ$ with the incident photon along the z-axis (i.e. $\bar{\theta}_i = 0^\circ$) places the photon scattering on the x–z plane resulting in

$$Y_{l0}(0, 0) = \left(\frac{2l+1}{4\pi} \right)^{1/2} \qquad Y_{lm}(0, 0) = 0 \qquad m \neq 0 \quad (14)$$

for the incident photon and

$$Y_{lm'}(\bar{\theta}_f, 0) = \left[\frac{2l+1}{4\pi} \frac{(l - |m'|)!}{(l + |m'|)!} \right]^{1/2} P_l^{m'}(x) \quad (15)$$

for the scattered photon, where $\bar{\theta}_f$ is the angle for the scattered photon, here $\bar{\theta}$ is the angle between the incident (on the z-axis) and scattered photons; thus $\bar{\theta} = \bar{\theta}_f$ and $x = \cos(\bar{\theta})$. Due to the assumptions about symmetry of the charge distribution, filled subshells and the scattering geometry, $m = m'$, the only nonzero terms remaining in equations (8) and (9) are

those which contain a product of $Y_{lm}(0,0)\cdot Y_{lm}(\bar{\theta}_f,0)$ in which $m=0$. Also due to $m+q=M$ (see the text below equation (7)), only terms in which $q=M$ are nonzero. Thus substitution of equations (14) and (15) into equation (7), where $\hat{\varepsilon}_q\cdot\hat{\varepsilon}^*_{q'}=\delta_{qq'}$ (see equation 5.9.7 in [16]) followed by the substitution of equation (7) into equations (8) and (9), results in the following formulae for magnetic and electric field form factor amplitudes

$$^{\mathrm{mag}}A^{f0}(E,\bar{\theta})=-r_o\varepsilon_i\varepsilon_j\sum_{pj}(2j+1)I^0_{pj}(E)\sum_{q=-1}^{1}P_j(x)(j01q|j1jq)^2 \tag{16}$$

$$^{\mathrm{el}}A^{f0}(E,\bar{\theta})=-r_0\varepsilon_i\varepsilon_j\sum_{pj}I^1_{pj}(E)\sum_{q=-1}^{1}[B_{qj}(\bar{\theta})+C_{qj}(\bar{\theta})+D_{qj}(\bar{\theta})]$$

$$B_{qj}(\bar{\theta})=B'_{qj}P_{j+1}(x)$$

$$B'_{qj}=j(2j+3)(j+1,01q|j+1,1jq)^2$$

$$C_{qj}(\bar{\theta})=C'_{qj}[P_{j+1}(x)+P_{j-1}(x)]$$

$$C'_{qj}=[j(j+1)(2j+3)(2j-1)]^{1/2}(j+1,01q|j+1,1jq)(j-1,01q|j-1,1jq)$$

$$D_{qj}(\bar{\theta})=D'_{qj}P_{j-1}(x)$$

$$D'_{qj}=(j+1)(2j-1)(j-1,01q|j-1,1jq)^2.$$

Here the energy-dependent radial integrals represented by $I^\lambda_{pj}(E)$ for $\lambda=0,1$ are given by

$$I^0_{pj}(E)=V_{pj}(E)\qquad I^1_{pj}(E)=\frac{(j+1)V_{pj-1}(E)+jV_{pj+1}(E)}{(2j+1)}. \tag{18}$$

When $q=0$, $(j010|j1j0)=0$ in equation (16). In equation (17) $B'_{0j}=D'_{0j}=j(j+1)$ and $C'_{0j}=-j(j+1)$, therefore $B_{0j}(\bar{\theta})+C_{0j}(\bar{\theta})+D_{0j}(\bar{\theta})=0$ for all j and $\bar{\theta}$. As a result the $q=0$ contribution in equations (16) and (17) is zero. Furthermore, due to the previously stated conditions, the $q=1$ and $q=-1$ terms in these two equations are equal. In equation (16), $(j011|j1j1)^2=(j01-1|j1j-1)^2=1/2$ and in equation (18) $B'_{1j}=B'_{-1j}=j^2/2$; $C'_{1j}=C'_{-1j}=j(j+1)/2$ and $D'_{1j}=D'_{-1j}=(j+1)^2/2$. As a result, equations (16) and (17) reduce to

$$^{\mathrm{mag}}A^{f0}(E,\bar{\theta})=-r_0\varepsilon_i\varepsilon_j\sum_{pj}(2j+1)I^0_{pj}(E)P_j(x) \tag{19}$$

for the magnetic field and to

$$^{\mathrm{el}}A^{f0}(E,\bar{\theta})=-r_0\varepsilon_i\varepsilon_j\sum_{pj}I^1_{pj}(E)[jP_{j+1}(x)+(j+1)P_{j-1}(x)] \tag{20}$$

for the electric field. The low **K** form factor amplitude can now be expressed compactly as

$$A^{f0}(E,\bar{\theta})=-r_0[\varepsilon_i\varepsilon_f]\sum_{pj}\{(2j+1)I^0_{pj}P_j(x)+I^1_{pj}(E)[jP_{j+1}(x)+(j+1)P_{j-1}(x)]\}. \tag{21}$$

2.4. Partitioning of A^{f0} into $A^{f0}_\perp$ and $A^{f0}_\parallel$

A^{f0} can be partitioned into parallel $A_\parallel$ and perpendicular $A_\perp$ polarization vector amplitudes ($A_\parallel$, the x component and $A_\perp$, the y component of polarization) and is given by

$$[\varepsilon_i\varepsilon_f]A^{f0}(E,\bar{\theta})=\left[\varepsilon_i^\perp\varepsilon_f^\perp\right]A^{mf}_\perp(E,\bar{\theta})+\left[\varepsilon_i^\parallel\varepsilon_f^\parallel\right]A^{mf}_\parallel(E,\bar{\theta})\cos(\bar{\theta}). \tag{22}$$

This transformation can be verified by using recursion formulae for Legendre and associated Legendre polynomials (see appendix B). Similarly the Rayleigh S-matrix amplitude is given by (from [1, 2, 4])

$$[\varepsilon_i \varepsilon_f] A^{\mathrm{sm}}(E, \bar{\theta}) = \left[\varepsilon_i^{\perp} \varepsilon_f^{\perp}\right] A_{\perp}^{\mathrm{sm}}(E, \bar{\theta}) + \left[\varepsilon_i^{\parallel} \varepsilon_f^{\parallel}\right] A_{\parallel}^{\mathrm{sm}}(E, \bar{\theta}). \tag{23}$$

Here

$$A_{\parallel}(E, \bar{\theta}) = -r_0 \sum_{pj} \frac{(2j+1)}{2} \left[S(\bar{\theta}) G_{pj}^{1}(E) + T(\bar{\theta}) G_{pj}^{0}(E)\right] \tag{24}$$

and

$$A_{\perp}(E, \bar{\theta}) = -r_0 \sum_{pj} \frac{(2j+1)}{2} \left[S(\bar{\theta}) G_{pj}^{0}(E) + T(\bar{\theta}) G_{pj}^{1}(E)\right], \tag{25}$$

where $G_{pj}^{\lambda}(E)$ represents the energy dependent, scattering angle-independent part of the amplitude. In the case of the full S-matrix representation of Rayleigh scattering A^{sm}, $G_{pj}^{\lambda}(E) = X_{pj}^{\lambda}(E)$ ($X_{pj}^{\lambda}(E)$ is the X-amplitude, defined in [1, 14] for example) and in the case of the form factor amplitude A^{f0}, $G_{pj}^{\lambda}(E) = I_{pj}^{\lambda}(E)$, where $I_{pj}^{\lambda}(E)$ is given by equation (18). $S(\bar{\theta})$ and $T(\bar{\theta})$ composed of Legendre $P_j^0(x)$ and associated Legendre $P_j^2(x)$ polynomials are given by

$$S(\bar{\theta}) = P_j^0(x) - \frac{P_j^2(x)}{j(j+1)} \tag{26}$$

$$T(\bar{\theta}) = \frac{P_{j-1}^0(x) + P_{j+1}^0(x)}{2} + \frac{P_{j-1}^2(x) + P_{j+1}^2(x)}{2j(j+1)}. \tag{27}$$

2.5. *Comparison between A^{sm}, A^{f0} and $f(q)$; correction of $\bar{\theta}$ dependence of A^{f0}*

The energy-dependent components of A^{sm} and A^{f0}, $X^{\lambda}(E)$ and $I^{\lambda}(E)$ respectively approach convergence with each other as the photon energy increases, but differ greatly at low energies especially at energies at which resonances occur (this will be illustrated in the results and discussion section). Due to the low **K** approximation the $\bar{\theta}$ dependence of A^{sm} and A^{f0} differ by the presence of $\cos(\bar{\theta})$ in the $A_{\parallel}$ part of A^{f0} in equation (22), but not present in A^{sm}, equation (23). Clearly in the limits of high E and low **K**, which leads to a small $\bar{\theta}$, the angle-dependent component of A^{f0} is very close to that for A^{sm}.

The connection between A^{f0} and $f(q)$ is illustrated by demonstrating that $f(q)$ can be factored out of the expression for A^{f0} simply by dividing it by $r_0[1+\cos^2(\bar{\theta})]$. This can be done because $A^{f0} = A_{\perp}^{f} + \cos(\bar{\theta}) A_{\parallel}^{f}$, where $A_{\perp}^{f} = r_0 f(q)$, and $A_{\parallel}^{f} = \cos(\bar{\theta}) A_{\perp}^{f} = r_0 \cos\bar{\theta}\, f(q)$ [5, 14], which yields

$$[\varepsilon_i \varepsilon_f] f(q) = [\varepsilon_i \varepsilon_f] A_{\perp}^{f}(E, \bar{\theta}) = A^{f0}(E, \bar{\theta}) / r_0 (1 + \cos^2\bar{\theta}). \tag{28}$$

Equations (1) and (28) for $f(q)$ always yield the same numerical values. However if one is interested in a multipole decomposed A^f and A^{asf} valid at all $\bar{\theta}$, it becomes necessary to replace the angle-dependent part of A^{f0} with that for A^{sm}. This can be achieved by substitution of $A_{\perp}^{f}$ and $A_{\parallel}^{f}$ into equation (23) in place of $A_{\perp}^{\mathrm{sm}}$ and $A_{\parallel}^{\mathrm{sm}}$ yielding a form factor amplitude designated by A^f, which has the same angle dependence as A^{sm}. Alternatively one can replace X_{pj}^{λ} by I_{pj}^{λ} (in equation (23)) and obtain a form factor amplitude in which each of its multipoles has the same angle dependence as those of A^{sm}, $[\varepsilon_i \varepsilon_j] A^f(E, \bar{\theta}) = \left[\varepsilon_i^{\perp} \varepsilon_f^{\perp}\right] A_{\perp}^{f}(E, \bar{\theta}) + \left[\varepsilon_i^{\parallel} \varepsilon_f^{\parallel}\right] A_{\parallel}^{f}(E, \bar{\theta})$, which is what was done for calculations illustrated in this paper. This makes it possible to calculate single multipole contributions to A^{asf} for a given subshell (i.e. $A_{pj}^{\mathrm{asf}} = A_{pj}^{\mathrm{sm}} - A_{pj}^{f}$).

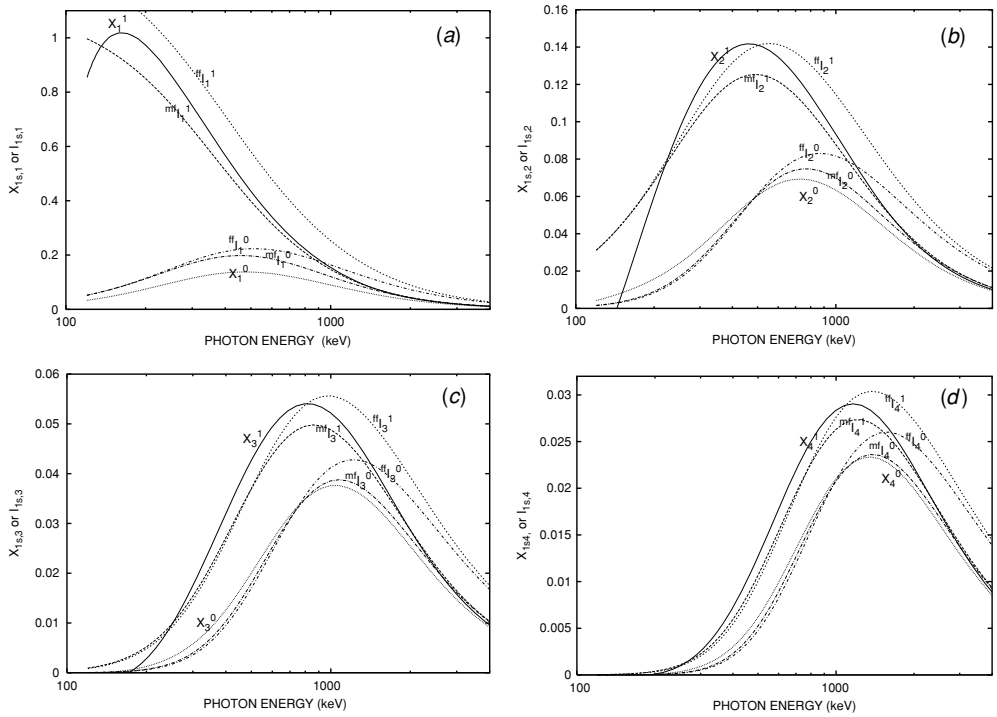

Figure 1. First four multipole amplitudes in $X^{\lambda}_{pj}(E)$, ${}^{mf}I^{\lambda}_{pj}(E)$ and ${}^{ff}I^{\lambda}_{pj}(E)$, respectively: where j corresponds to the 2^j-pole and $\lambda = 0, 1$ to magnetic and electric field multipoles respectively and $p = 1s_{1/2}$. All calculations were done using the Dirac–Slater potential. Uranium atom, $Z = 92$; subscript p is omitted in all graphical labels (applies to all graphs in this paper). In all four graphs, X^1_j corresponds to the dark solid line; ${}^{mf}I^1_j$ to the dark dashed line; ${}^{ff}I^1_j$ to the dotted line; X^0_j to the finely dotted line; ${}^{mf}I^0_j$ to the dot-dash line and ${}^{ff}I^0_j$ to the fine dot-dash line. (*a*) $j = 1$; (*b*) $j = 2$; (*c*) $= 3$; (*d*) $j = 4$.

3. Results and discussion

3.1. Energy and scattering angle dependence of various S-matrix and form factor amplitudes

The form factor amplitude, has been decomposed into subshells as well as the electric and magnetic field multipoles, such that it can be expressed in the same form as the decomposed S-matrix elastic photon scattering amplitude $A^{\rm sm}$. In this discussion, when $H_p(r) = [|E_p| - V(r)]^{-1}$, A^f will be referred to as the modified form factor amplitude designated by A^{mf}, if the $\bar{\theta}$ dependence is correct and by A^{mf0} if the $\mathbf{K} \to 0$ approximation is in effect. When $H_p(r) = 1$, A^f having the correct $\bar{\theta}$ dependence will be represented by A^{ff} or by A^{ff0} when $\mathbf{K} \to 0$. One can make a direct comparison between the multipoles of the X-amplitudes X^{λ}_{pj} (from $A^{\rm sm}$) and those of the form factor amplitude radial integral ${}^{f}I^{\lambda}_{pj}$ (from A^f). Such a comparison is given in figure 1 for the uranium K-shell, illustrating the photon energy dependence of X^{λ}_{pj} from $A^{\rm sm}_{pj}$, which is exact within IPA; the modified form factor radial integral ${}^{mf}I^{\lambda}_{pj}$ from A^{mf}_{pj} (has the same E dependence as in A^{mf0}_{pj}); and the form factor radial integral ${}^{ff}I^{\lambda}_{pj}$, from A^{ff}_{pj} (same E dependence as in A^{ff0}_{pj}). All calculations are done

within IPA using a Dirac–Slater potential. The K shell of a heavy atom was chosen because one can illustrate the largest possible differences between X^{λ}_{pj}, ${}^{mf}I^{\lambda}_{pj}$ and ${}^{ff}I^{\lambda}_{pj}$. A second reason is that as the scattering angle increases, the amplitude (i.e. A^{sm} and A^{f}) for whole atom photon scattering rapidly becomes dominated by contributions from the innermost shells.

Investigation of the first four electric and magnetic field multipole amplitudes over a photon energy range of 120 keV–4 MeV demonstrates that the X^{λ}_{pj} and ${}^{mf}I^{\lambda}_{pj}$ ($p = 1\mathrm{s}_{1/2}$ throughout this paper) curves are much closer to each other than is the ${}^{ff}I^{\lambda}_{pj}$ curve, the former two merging with increasing energy while the latter not merging with X^{λ}_{pj}. This result confirms that partial inclusion of the electron–nuclear Coulomb effects contained in H_p (equation (3)) provides for a much better form factor amplitude. These graphs show that the electric field dipole is dominant at energies below about 0.5 MeV for the uranium K-shell. However as the photon energy increases the number of significant magnetic and electric field multipoles increases. The differences between X^{λ}_{pj}, ${}^{mf}I^{\lambda}_{pj}$ and ${}^{ff}I^{\lambda}_{pj}$ beyond electric field dipole are nearly zero for a middle shell amplitude such as the $4\mathrm{s}_{1/2}$ subshell (in uranium). Even in the electric field dipole, the differences are very small except at energies at which resonances occur. The very small difference between ${}^{mf}I_j$ and ${}^{ff}I_j$ for all j is expected since Coulomb effects are relatively small for middle subshells. The differences between X^{λ}_{pj}, ${}^{mf}I^{\lambda}_{pj}$ and ${}^{ff}I^{\lambda}_{pj}$ decrease as one goes from inner to outer shells in a given atom as well as going to lower Z for the same subshell.

Figure 2 illustrates the energy dependence of the first four multipoles of A^{sm}_{pj} using equation (23), of the modified form factor amplitude, A^{mf}_{pj} using equation (23) but replacing X^{λ}_{pj} by ${}^{mf}I^{\lambda}_{pj}$ and of A^{mf0}_{pj} using equation (21) which is equivalent to equation (22). These results are for the K-shell of uranium with a scattering angle $\bar{\theta} = 50^{\circ}$. For simplicity the product of polarization magnitudes $\varepsilon^{\perp}_{i}\varepsilon^{\perp}_{f}$ and $\varepsilon^{\parallel}_{i}\varepsilon^{\parallel}_{j}$ were taken to be unity giving $A_{\perp}$ and $A_{\parallel}$ equal weight and r_0 is not included in the amplitudes (same applies to all subsequent figures). Here the A^{sm}_{pj} and A^{mf}_{pj} curves are very close at energies above 0.5 MeV and almost merge at 4.0 MeV. From this graph, as well as from figure 1, it is clear that the higher the multipole, the higher is the energy at which the amplitude for a given multipole reaches its maximum.

3.2. Validity of the low momentum transfer approximation in A^{mf0}

The curves for the A^{mf0} and A^{mf} amplitudes for the uranium K-shell are the same at $\bar{\theta} = 0$, where $A_{\perp} = A_{\parallel}$ and differ by as much as about 25% in the range $0^{\circ} \leqslant \bar{\theta} \leqslant 90^{\circ}$. At 90° the difference is virtually zero because $A_{\parallel} \approx 0$, but as $\bar{\theta}$ increases above 90° the difference between these two amplitudes increases rapidly, because $|A_{\parallel}|$ now increases approaching $|A_{\perp}|$ in magnitude while $\cos\bar{\theta}$ has changed sign. These trends are reflected in the energy dependence of the total amplitudes $A^{\mathrm{sm}}_{p} = \sum_j A^{\mathrm{sm}}_{pj}$, $A^{mf}_{p} = \sum_j A^{mf}_{pj}$ and $A^{mf0}_{p} = \sum_j A^{mf0}_{pj}$ at $\bar{\theta} = 25^{\circ}$, 50°, 90° and 150° shown in figure 3. At 25° all three curves are very close, with the maximum difference between A^{mf} and A^{mf0} of less than 5%, occurring at the lowest energies. The differences between all three amplitudes in the angle range $0^{\circ} \leqslant \bar{\theta} \leqslant 90^{\circ}$ are very small at energies greater than about 0.5 MeV. These results are of interest if one intends to demonstrate that the form factor amplitude can be derived from the S-matrix formalism. Such a derivation can be accomplished by imposing the low momentum transfer condition to the nonexponential part of the S-matrix element to make it possible for the Dirac α matrix containing terms to cancel out (see equation (3) and Goldberger equation (2.7) Zhou [15, p 49] or appendix A). Comparison of equations (22) and (23) reveals that such a form factor amplitude (A^{f0}) has the wrong angle dependence. Despite this, A^{f0} (includes A^{mf0} and A^{ff0}) is a fairly good approximation to A^{f} (includes A^{mf} and A^{ff}) at high energy, when $\theta \leqslant 90^{\circ}$.

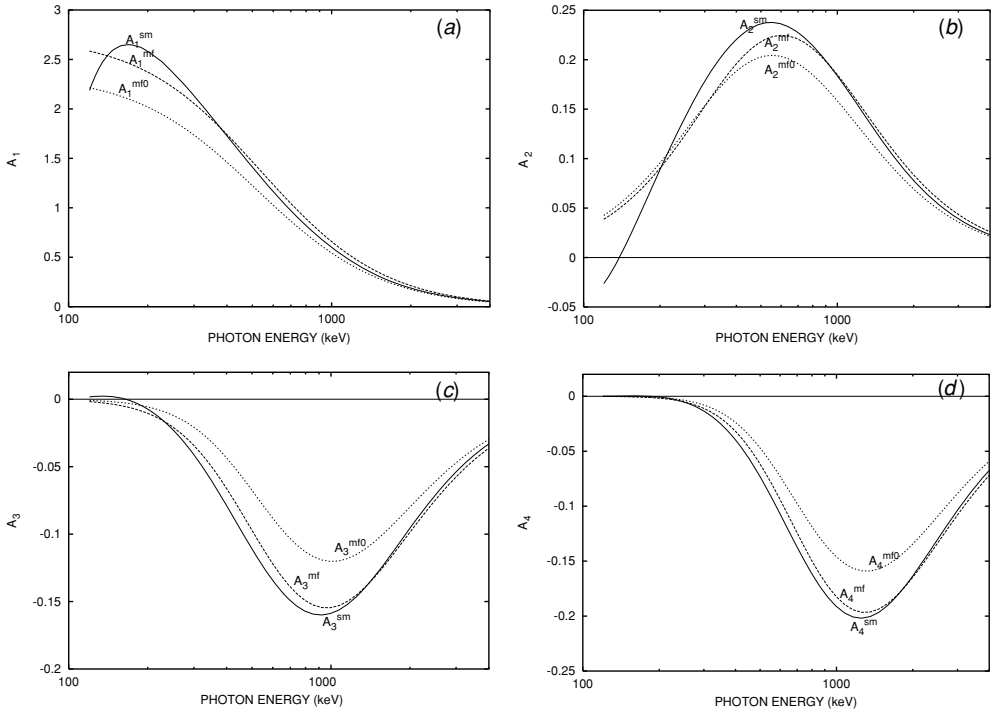

Figure 2. First four multipoles of elastic photon scattering amplitudes: $A^{\rm sm}_{pj}(E,\bar\theta)$ is obtained from equation (23); $A^{mf}_{pj}(E,\bar\theta)$ is also obtained from equation (23), but $X^{\lambda}_{pj}(E)$ is replaced by ${}^{mf}I^{\lambda}_{pj}(E)$; and $A^{mf0}_{pj}(E,\bar\theta)$ is obtained from equation (21). Uranium atom, $p = 1s_{1/2}$, $\bar\theta = 50^\circ$. Polarization magnitudes are taken to be unity and r_0 is omitted, resulting in a unitless amplitude comparable to the form factor $f(q)$ (same applies to all subsequent graphs in the paper). (*a*) $j = 1$; (*b*) $= 2$; (*c*) $j = 3$; (*d*) $j = 4$.

Furthermore one can obtain the form factor $f(q)$ (equation (1)) from the S-matrix formalism by simply dividing A^{f0} by $r_0(\cos^2\bar\theta + 1)$ (see equation (28)).

3.3. Behaviour of Re $A^{\rm asf}$ *and* Re $A^{\rm asf}_j$

The real part of the anomalous scattering factor Re $A^{\rm asf}_{pj} = \left[\text{Re}\, A^{\rm sm}_{pj} - A^{mf}_{pj}\right]$ up to the first four multipoles, as well as the total Re $A^{\rm asf}$ summed over the first 32 multipoles is shown in figure 4. These amplitudes pertain to the K-shell of uranium at scattering angles of 0°, 50°, 100° and 150°. In this particular case the relative dipole contribution to $A^{\rm asf}$ at lower energy appears to be greater at small angles, while at larger angles, higher multipole contributions become more substantial, especially at $\bar\theta = 150^\circ$, where even the third and fourth multipoles contribute significantly. Note that at all angles, $A^{\rm asf}$ is nearly zero at about 2 MeV, while $A^{\rm asf}_j$ is still of significant magnitude especially at large angles. Here the $A^{\rm asf}_j$ s appear to cancel each other out resulting in $A^{\rm asf}$ converging to zero faster than the individual $A^{\rm asf}_j$. Aside from the resonances, the beyond dipole contribution to the uranium $4s_{1/2}$ shell $A^{\rm asf}$ is nearly negligible at all angles. The same is true for all higher atomic levels. Only up to quadrupole $A^{\rm asf}_j$ are significant for the K-shell of a light atom like Ca (figure 5) and only dipole electric field A^{mf}_j for an L shell or higher level.

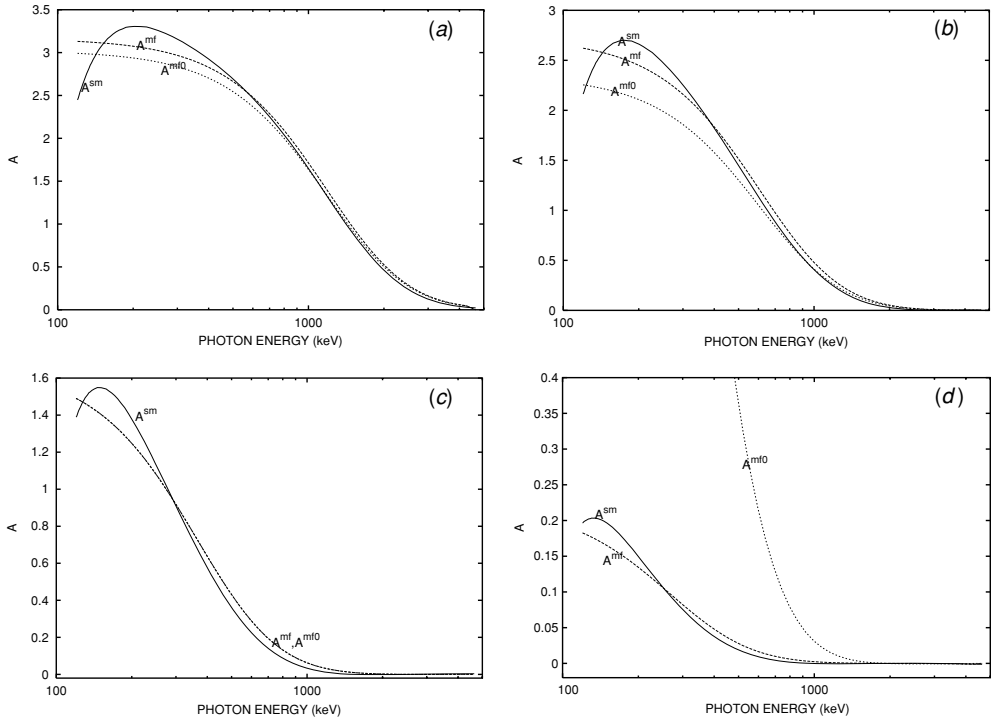

Figure 3. Angle and energy dependence of total elastic photon scattering amplitudes: $A_p^{\rm sm}(E,\bar\theta) = \sum_j^n A_{pj}^{\rm sm}(E,\bar\theta)$, $A_p^{mf}(E,\bar\theta) = \sum_j^n A_{pj}^{mf}(E,\bar\theta)$ and $A_p^{mf0}(E,\bar\theta) = \sum_j^n A_{pj}^{mf0}(E,\bar\theta)$. Uranium atom, $p = 1s_{1/2}, n = 32$, units correspond to amplitudes in figure 2. (*a*) $\bar\theta = 25^\circ$; (*b*) 50°; (*c*) 90° and (*d*) 150°.

As the photon energy increases, the magnitude of $A^{\rm sm}$ decreases approaching zero as does $A^{\rm asf}$. However, one may ask if the magnitude of $A^{\rm asf}$ relative to $A^{\rm sm}$, given by $\bar A^{\rm asf} = A^{\rm asf}/A^{\rm sm}$ also approaches zero with increasing E. Here $\bar A^{\rm asf}$ does in fact approach zero for all shells of light atoms like Ca and for middle and outer shells of heavy atoms, but it increases for the inner shells of heavy atoms especially at large angles. For example $\bar A^{\rm asf}$ is about 0.8 in the case of the K-shell of uranium at $E = 1.0$ MeV and $\bar\theta = 90^\circ$, at the same energy it is only about 0.04 at $\bar\theta = 25^\circ$, but exceeds 4.0 at $\theta = 150^\circ$. These results are consistent with the results reported in [5] where the relative difference between the S-matrix and the modified form factor total atom differential cross sections can increase with increasing $\bar\theta$ exceeding 100% when $\bar\theta = 90^\circ$. This behaviour is most likely due to $A_j^{\rm asf}$ not quite converging to zero with increasing energy. This may be due to omission of $c(\bar{\mathbf{K}}\cdot\mathbf{P})$ in relevant equations from (3) to (22). Since as one goes to higher Z and to inner shells, the electron momentum $\mathbf{P}$ will increase, this along with increasing momentum transfer would cause $\bar{\mathbf{K}} = \mathbf{K_i} \approx \mathbf{K_f}$ to no longer apply, at finite $\hat\theta$, resulting in a greatly enhanced $c(\bar{\mathbf{K}}\cdot\mathbf{P})$ contribution to $A^{\rm asf}$, thereby increasing $\bar A^{\rm asf}$.

4. Summary

The modified form factor (including the form factor) amplitude has been decomposed into subshell components as well as an infinite sum of electric and magnetic field multipoles by

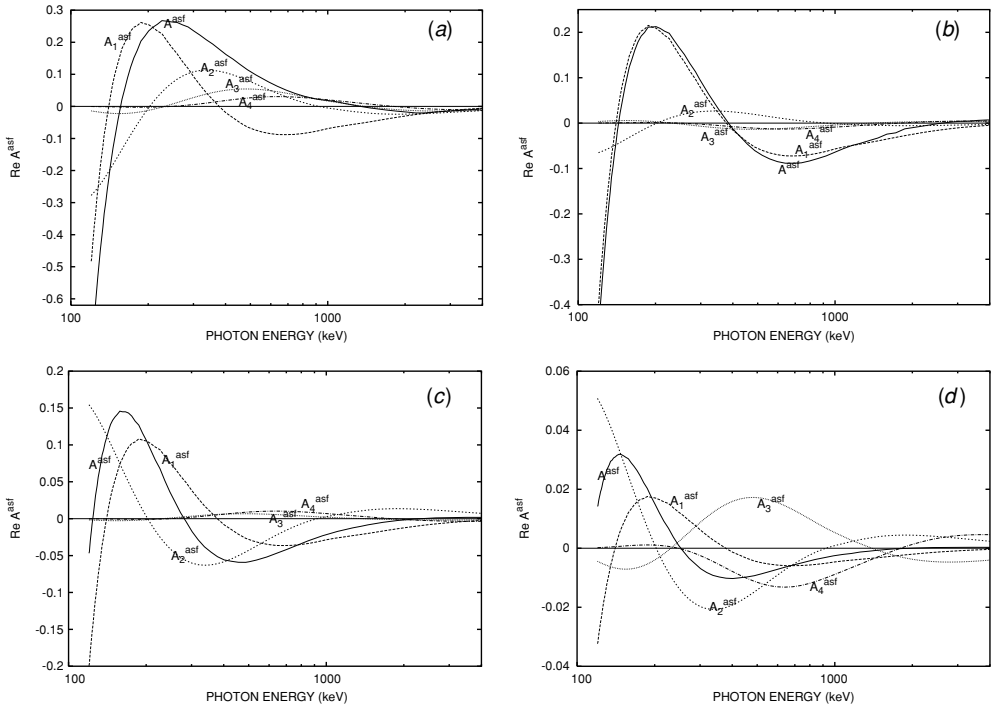

Figure 4. First four multipoles and total amplitude of the real component of the anomalous scattering factor: the jth multipole contribution $\mathrm{Re}\, A_{pj}^{\mathrm{asf}}(E,\bar{\theta}) = [\mathrm{Re}\, A_{pj}^{\mathrm{sm}}(E,\bar{\theta}) - A_{pj}^{mf}(E,\bar{\theta})]$ and total amplitude $\mathrm{Re}\, A_{p}^{\mathrm{asf}}(E,\bar{\theta}) = \sum_j^n [\mathrm{Re}\, A_{pj}^{\mathrm{sm}}(E,\bar{\theta}) - A_{pj}^{mf}(E,\bar{\theta})]$. Uranium atom, $n = 32$, $p = 1s_{1/2}$, units same as in figures 2 and 3. A^{asf} corresponds to the solid line; A_1^{asf} to the dark dashed line; A_2^{asf} to the dark dotted line; A_3^{asf} to the finely dotted line; and A_4^{asf} to the dot-dash line. (*a*) $\bar{\theta} = 0^\circ$; (*b*) 50°; (*c*) 100°; and (*d*) 150°.

starting with equation (3) in the high energy limit of A^{sm} at low momentum transfer ($\mathbf{K} \approx 0$). Omission of $c(\bar{\mathbf{K}} \cdot \mathbf{P})$ yields the low $\mathbf{K}$ form factor amplitude A^{f0}. By assuming that the charge density is spherically symmetrical, a very simple expression results for $A^{f0} = \sum_j A_j^{f0}$ (equation (22)).

The limited accuracy of equation (21) with respect to $\bar{\theta}$ dependence is quite clear, when it is expressed in terms of $A_\perp$ and $A_\parallel$ as given by equation (22). Comparison of equation (22) to that for A^{sm}, represented by equation (23) shows that the only difference in angle dependence is the additional $\cos\bar{\theta}$ in equation (22), therefore $[A^f(E,\mathbf{K}) - A^{f0}(E,\mathbf{K})]$ approaches zero as $\bar{\theta} \to 0^\circ$. However this is still a fairly good approximation at high photon energies when $\theta \leqslant 90^\circ$.

A^{asf} can become quite large at lower E for the innermost shells of heavy atoms, but it decreases rapidly with increasing n and decreasing Z, where the major contribution to A^{asf} for middle and outer shells is due to resonances. However such resonance effects decrease with increasing multipolarity. At energies up to about ten times the K-shell binding energy only up to quadrupole A_j^{asf} for light atoms like Ca and for atoms as heavy as uranium only up to the fourth multipole of A_j^{asf} are needed for an accurate A^{asf}. The relative size of the individual multipole contributions to the total amplitude increase with increasing $\bar{\theta}$ especially at $\bar{\theta} > 120^0$, but such effects partly cancelled out.

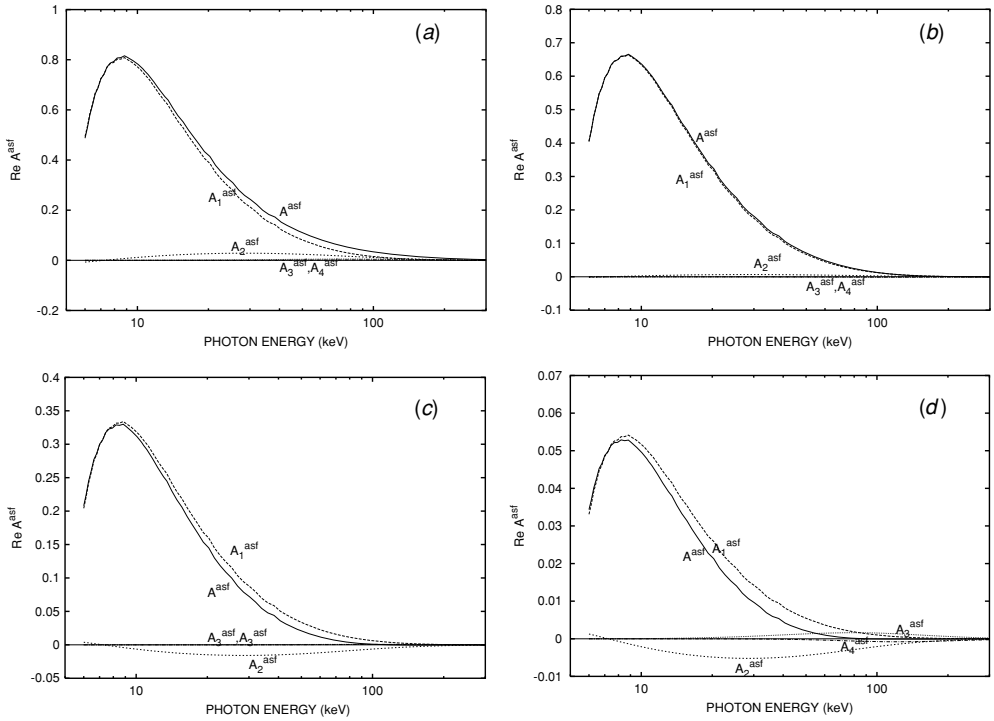

Figure 5. Same as figure 4 but for Ca ($Z = 20$).

Although anomalous scattering factors are usually obtained from photoionization cross sections, only accurate at forward angle scattering (see references in [8, 9]) it is possible to derive an $A^{\rm asf}$ that is accurate at all angles. This was done for the nonrelativistic K-shell case [8, 9]. The decomposition of $A^{\rm asf}$ outlined in this paper can serve as a test for various levels of generality. For example one can test the validity of a new formula for a relativistic angle-dependent $A^{\rm asf}(E, \bar{\theta})$ first in the electric field dipole approximation, then one may go to progressively higher multipoles (electric and magnetic) and test them. Also one may start with an $A^{\rm asf}$ for the K-shell then go to higher shells testing possible formulations to predict contributions from each subshell. Finally the derivations presented in this paper demonstrate that the form factor $f(q)$ can be derived from the second order S-matrix formalism in the limit of high photon energy and low momentum transfer.

Appendix A

Taken from Zhou (p 49 in [15]). High energy and low momentum transfer limit of $A^{\rm sm}$

$$A_p^{\rm sm} = \frac{r_0 c^2}{2}\left[\left\langle p\left|e^{i\mathbf{K}\cdot\mathbf{r}}\frac{(\alpha\cdot\varepsilon_{\mathbf{f}})(1+\alpha\cdot\mathbf{K_i})(\alpha\cdot\varepsilon_{\mathbf{i}})}{|E_p|-V-c(\mathbf{K_i}\cdot\mathbf{P})}\right|p\right\rangle + \langle p\left|e^{i\mathbf{K}\cdot\mathbf{r}}\frac{(\alpha\cdot\varepsilon_{\mathbf{i}})(1+\alpha\cdot\mathbf{K_f})(\alpha\cdot\varepsilon_f)}{|E_p|-V-c(\mathbf{K_f}\cdot\mathbf{P})}\right|p\right\rangle\right] \tag{A.1}$$

Using

$$(\alpha\cdot\mathbf{A})(\alpha\cdot\mathbf{B})+(\alpha\cdot\mathbf{B})(\alpha\cdot\mathbf{A}) = 2(\mathbf{A}\cdot\mathbf{B}) \tag{A.2}$$

and assuming a small momentum transfer $\bar{\mathbf{K}} \approx \mathbf{K_i} \approx \mathbf{K_f}$ in the limit $E \to \infty$ and averaging over electron spin, one obtains

$$A_p^{\mathrm{sm}} \simeq r_o mc^2 [\varepsilon_{\mathbf{i}} \cdot \varepsilon_{\mathbf{f}}^*] \left[\left\langle p \left| \frac{\mathrm{e}^{-\mathrm{i}\mathbf{K}\cdot\mathbf{r}}}{|E_p| - V - c(\bar{\mathbf{K}} \cdot \mathbf{P})} \right| p \right\rangle \right]. \tag{A.3}$$

Appendix B

Equation (22) can be verified by deriving equation (21) from equations (22), (24)–(27). First it will be shown that the magnetic field amplitude form factor equation (19) is equal to

$${}^{\mathrm{mag}}A_{pj}^{f0}(E,\bar{\theta}) = {}^{\mathrm{mag}}A_{\perp,pj}^{f}(E,\bar{\theta}) + x\left[{}^{\mathrm{mag}}A_{\parallel,pj}^{f}(E,\bar{\theta})\right], \tag{B.1}$$

where $x = \cos(\bar{\theta})$. Substitution of equations (26) and (27) into (24) and (25) with subsequent substitution of the latter two equations into (B.1) and setting $G_{pj}^0 = I_{pj}^0$ (discarding all $\lambda = 1$ terms) yields

$$\begin{aligned} {}^{\mathrm{mag}}A_{pj}^{f0}(E,\bar{\theta}) = \frac{-r_0}{2}(2j+1)I_{pj}^0(E) \Bigg\{ & P_j^0(x) - \frac{P_j^2(x)}{j(j+1)} \\ & + \frac{x}{2}\left(P_{j-1}^0(x) + P_{j+1}^0(x) + \frac{P_{j-1}^2(x) + P_{j+1}^2(x)}{j(j+1)} \right) \Bigg\}. \end{aligned} \tag{B.2}$$

The associated Legendre polynomials in (B.2) are eliminated by using Legendre's differential equation in the following form

$$P_l^2(x) = (1-x^2)P_l''(x) = 2xP_l^{0\prime}(x) - l(l+1)P_l^0(x) \tag{B.3}$$

setting $l = j$ as well as $l = j \pm 1$ and by substitution of the recursion

$$P_l^{0\prime}(x) = l\left(P_{l-1}^0(x) - xP_l^0(x)\right)(1-x^2)^{-1} \tag{B.4}$$

into (B.3) followed by the substitution of (B.3) into (B.2) yields

$$\begin{aligned} {}^{\mathrm{mag}}A_{pj}^{f0}(E,\bar{\theta}) = -\frac{r_0}{2}(2j+1)I_{pj}^0(E) \Bigg\{ & 2P_j^0(x) - \frac{2jx\left[P_{j-1}^0(x) - xP_j^0(x)\right]}{j(j+1)(1-x^2)} \\ & + \frac{x}{j(j+1)(1-x^2)}\left[(1-x^2)\left[jP_{j-1}^0(x) - (j+1)P_{j+1}^0\right]\right. \\ & \left. + (j-1)x\left[P_{j-2}^0 - xP_{j-1}^0(x)\right] + (j+1)x\left[P_j^0(x) - xP_{j+1}^0(x)\right] \right\}. \end{aligned} \tag{B.5}$$

Then substitution of the recursion $(j-1)P_{j-2}^0(x) = (2j-1)xP_{j-1}^0(x) - jP_j^0(x)$ and $(j+1)P_{j+1}^0(x) = (2j+1)xP_j^0(x) - jP_{j-1}^0(x)$ into (B.5) results in

$$\begin{aligned} {}^{\mathrm{mag}}A_{pj}^{f0}(E,\bar{\theta}) = -r_o(2j+1)I_{pj}^0(E) \Bigg\{ & P_j^0(x) - \frac{x\left[P_{j-1}^0(x) - xP_j^0(x)\right]}{(j+1)(1-x^2)} \\ & + \frac{x\left[P_{j-1}^0(x) - xP_j^0(x)\right]}{(j+1)(1-x^2)} \Bigg\} = -r_0(2j+1)I_{pj}^0(E)P_j^0(x) \end{aligned} \tag{B.6}$$

which agrees with equation (19). The electric field form factor amplitude (equation (21)) can be derived from

$${}^{\mathrm{el}}A_{pj}^{f0}(E,\bar{\theta}) = {}^{\mathrm{el}}A_{\perp,pj}^{f}(E,\bar{\theta}) + x\left[{}^{\mathrm{el}}A_{\parallel,pj}^{f}(E,\bar{\theta})\right] \tag{B.7}$$

starting with equations (24) and (25), but only taking the $G_j^1 = I_j^1$ containing terms gives

$$ {}^{\mathrm{el}}A_{pj}^{f0}(E,\bar{\theta}) = \frac{-r_0}{2}(2j+1)I_{pj}^1(E)\left\{xP_j^0(x) - \frac{xP_j^2(x)}{j(j+1)} + \frac{1}{2}\left(P_{j-1}^0(x) + P_{j+1}^0(x) + \frac{P_{j-1}^2(x) + P_{j+1}^2(x)}{j(j+1)}\right)\right\}. \tag{B.8} $$

The only difference between the angle-dependent parts of equations (B.2) and (B.8) is that x is moved from the last three terms in brackets to the first two. This is because those two terms in equation (B.8) correspond to the electric field component of $A_\parallel$, while the first three terms in equation (B.2) correspond to the magnetic field component of $A_\parallel$. Then repeating the steps taken to derive equation (B.6) from (B.2) yields

$$ {}^{\mathrm{el}}A_{pj}^{f0}(E) = -r_o(2j+1)I_{pj}^1(E)\left[xP_j^0(x) + \frac{\left[x^2 - P_{j-1}^0(x) + xP_j^0(x)\right] + \left[P_{j-1}^0(x) - xP_j^0(x)\right]}{(j+1)(1-x^2)}\right. \tag{B.9} $$

and after cancellation of terms equation (B.9) reduces to

$$ {}^{\mathrm{el}}A_{pj}^{f0}(E) = -r_0\sum_j \frac{(2j+1)}{(j+1)}I_{pj}^1(E)\left[jxP_j^0(x) + P_{j-1}^0(x)\right]. \tag{B.10} $$

Finally, substitution of the recursion $(2j+1)xP_j^0(x) = (j+1)P_{j+1}^0 + jP_{j-1}^0(x)$ into equation (B.10) results in equation (20) given by ${}^{\mathrm{el}}A_{pj}^{f0}(E,\bar{\theta}) = -r_0\sum_{pj} I_j^1(E)\left[jP_{j+1}^0(x) + (j+1)P_{j-1}^0(x)\right]$.

References

[1] Johnson W R and Feiock F D 1968 *Phys. Rev.* **168** 22
[2] Akhieser A I and Berestskii V B 1965 *Quantum Electrodynamics* (New York: Interscience)
[3] Lin K, Cheng K and Johnson W R 1975 *Phys. Rev.* A **11** 1946
[4] Kissel L, Pratt R H and Roy S C 1980 *Phys. Rev.* A **22** 1970
[5] Kissel L, Zhou B, Roy S C, Sen Gupta S K and Pratt R H 1995 *Acta Cryst.* A **51** 271
[6] Zhou B, Kissel L and Pratt R H 1992 *Phys. Rev.* A **45** 2983
[7] Smith D Y 1987 *Phys. Rev.* A **35** 3381
[8] Bergstrom P M, Kissel L, Pratt R H and Costescu A 1997 *Acta Cryst.* A **53** 7
[9] Costescu P M, Bergstrom P M, Dinu C and Pratt R H 1994 *Phys. Rev.* A **50** 1390
[10] LaJohn L A and Pratt R H 1998 *Phys. Rev.* A **58** 4989
[11] Dias E W B *et al* 1997 *Phys. Rev. Lett.* **78** 4553
Hanson D L, Hemmers O, Wang H, Lindle D W, Focke P, Sellin I A, Heske C, Chakraborty H S, Deshmuka P C and Manson S T 1999 *Phys. Rev.* A **60** 1641
[12] Dolmatov V K and Manson S T 2001 *Phys. Rev.* A **63** 0222704
Dolmatov V K, Balyenkov A S and Manson S T 2001 *Phys. Rev.* A **64** 042718
[13] Dolmatov V K, Bailey D and Manson S T 2005 *Phys. Rev.* A **72** 022718
Dolmatov V K, Balyenkov A S and Manson S T 2003 *Phys. Rev.* A **67** 062714
Hopersky A N, Nadolinsky A M and Yarha V A 2005 *J. Exp. Theor. Phys.* **101** 597
[14] Kane P P, Kissel L, Pratt R H and Roy S C 1986 *Phys. Rep.* **140** 77
Kissel L 1977 *PhD Thesis* University of Pittsburgh, Pittsburgh, PA
[15] Goldberger M L and Low F E 1968 *Phys. Rev.* **176** 1778
Zhou B 1991 *PhD Thesis* University of Pittsburgh
[16] Edmonds A R 1957 *Angular Momentum in Quantum Mechanics* (Princeton, NJ: Princeton University Press)